

Investigation of the behavior of hydrogen-bonded phenolic compounds and their determination by using poly(vinylferrocenium)-polyaniline composite film

Muammer Kavanoz,¹ Nuran Özçiçek Pekmez,² Muzaffer Can³

¹Department of Chemistry, Recep Tayyip Erdogan University, 53100 Rize, Turkey

²Department of Chemistry, Hacettepe University, 06800 Beytepe/Ankara, Turkey

³Department of Chemistry, Kırıkkale University, 71450 Kırıkkale, Turkey

Correspondence to: N. Ö. Pekmez (E-mail: npekmez@hacettepe.edu.tr)

ABSTRACT: The hydrogen bonding between phenolic compounds (phenol (Ph), catechol (Ct), resorcinol (Rs), and hydroquinone (Hq)) is investigated at pH 4. The oxidation behaviors of total phenolic compounds (TotPh) are different from their individual behaviors due to the existence of intermolecular hydrogen-bonded oligomeric clusters. Theoretical calculations and voltammetric and spectroscopic evidences support the intermolecular hydrogen bonding. The interaction of the phenolic compounds with polyaniline (PANI) and poly(vinylferrocenium) (PVF⁺) films are also investigated electrochemically and spectroscopically. The phenolic molecules are immobilized in both polymers due to the construction of hydrogen bonds by PANI and the complexation with PVF⁺. In addition, Ct and Hq are catalytically oxidized by PANI. Determinations of Ct and TotPh are performed on PVF⁺-PANI composite-coated Pt electrode using amperometric *I-t* method. Composite coating exhibits significant electrochemical activity toward Ct and TotPh, with high sensitivity and a wide linearity range. The steady-state currents versus concentration of Ct and TotPh are found to be linear in the range of 1.35×10^{-3} –50.0 mM and 4.10×10^{-4} –560 mM for two linear regions, respectively. © 2016 Wiley Periodicals, Inc. *J. Appl. Polym. Sci.* **2016**, *133*, 43596.

KEYWORDS: coatings; composites; conducting polymers; electrochemistry; spectroscopy

Received 24 October 2015; accepted 3 March 2016

DOI: 10.1002/app.43596

INTRODUCTION

Hydrogen bonds are relatively weak interactions between molecules and yet they are of paramount importance in chemistry and pivotal in determining biomolecular structure and function.¹ This type of interaction governs many biologically important processes in which the enzymatic catalysis is particularly relevant.^{2,3} R. Vianello *et al.* performed a comparative spectroscopic study and a computational study of the vibrational OH stretching frequencies in liquid ethanol–ethanol and liquid ethanol–*N*-methylimidazole dimers.⁴ The latter system mimics the hydrogen bond formation between serine and histidine residues, which is the incipient step in the enzymatic activity of the catalytic triads. Hydrogen bonding is one mechanism for the sorption of organic compounds on carbon-based sorbents and amine-modified hyper-cross-linked polymeric adsorbent.^{5,6} The –OH substitution on the phenolic and the hydroxyl/carboxylic groups on the carbon nanotube (CNT) surface may form

hydrogen bonds that may also be formed between surface-adsorbed and dissolved phenolic.⁷

In the family of conducting polymers, PANI has been one of the most studied conducting polymers, on account of its ease of synthesis, high electrical conductivity, good redox reversibility, environmental stability, simple doping/dedoping chemistry, and its ability to catalyze electrochemical redox reactions of some inorganic ions and organic compounds.⁸ PANI can be used as a mediator in the electrocatalytic field such as Fe^{2+/3+},⁹ and hydroquinone/benzoquinone.¹⁰ Ferrocene and its derivatives are the most frequently studied modifiers of electrodes as they possess an electroactive ferrocenyl group that displays rapid heterogeneous electron transfer rates. Similarly, PVF⁺-modified electrode has received much attention mainly due to its interesting redox characteristics and its application as an electrocatalyst and a sensor.¹¹ PVF⁺-coated electrode was found to catalyze the electro-oxidation and electroreduction of some organic species

Additional Supporting Information may be found in the online version of this article.

© 2016 Wiley Periodicals, Inc.

such as anthracene in acetonitrile and the electro-oxidation of H_2O_2 in aqueous solution.¹² Furthermore, it was demonstrated that this coating could be used as a preconcentration agent for the analysis of some anions in aqueous medium.¹³ In our previous studies, PVF^+ -PANI composite-coated electrode was electrochemically prepared on Pt electrode for combining electrocatalytic properties of an intrinsically conducting polymer and a redox polymer. PANI and PVF^+ polymers were codeposited from a methylene chloride solution, containing PVF polymer and aniline monomer.¹⁴

Phenolic compounds are widely dispersed in natural water and wastewater due to numerous contaminants released by industrial processes of plastics, natural degradation of humic and lignocellulosic substances, as well as paints, photographic chemicals, pharmaceutical preparations, pesticides, resins, antioxidants, paper, and cellulose.¹⁵ These are scattered over a broad area, which result in serious environmental concerns because of their toxicity, low biodegradability, and their ability to build up potential in plants and tissues. To give an example, fish living in polluted lakes and streams are exposed to these compounds which cause an unfavorable odor and taste in both lakes and fish. They are considered by both the US Environmental Protection Agency (EPA) and the European Union (EU) to be the primary pollutants to the environment as a result of their uses.^{16,17} To determine these toxic compounds, some instrumental techniques such as gas, liquid chromatography, capillary electrochromatography, and spectrophotometry are used which give sensitive and reliable results.^{18–20} However, these instrumental methods are expensive, time-, and reagent-consuming and have numerous co-existent interferences. Therefore, it is of utmost importance to develop a sensitive analytical method for the determination of phenolic compounds. Electrochemical methods, involving the development of chemical sensors and chemically modified electrodes have been utilized; motivations underlying the modification of the electrode surface are (i) improved electrocatalysis, (ii) absence of surface fouling, and (iii) prevention of undesirable reactions competing kinetically with the desired electrode process.²¹ Recently, there has been a tendency to use chemically modified electrodes with and without bacteria to electrochemically determine phenolic compounds.^{22–24} Biosensors, based on immobilized peroxidases, such as horseradish peroxidase,²⁵ polyphenol oxidase, or tyrosinase²⁶ have been used for phenol detection.

In this study, the influence of the hydrogen bonds on electrochemical and spectroscopic behaviors of phenolic compounds is investigated. The feasibility of the hydrogen bonding between PANI and phenolic molecules and among phenolic molecules is elucidated by theoretical calculation. The interaction of the phenolic compounds with PVF^+ homopolymer film is also investigated electrochemically and spectroscopically. Eventually, amperometric determinations of Ct and TotPh are examined by using PVF^+ -PANI composite-coated electrode because of the importance of their quantitative analysis in pharmaceuticals and environmental areas, respectively.

EXPERIMENTAL

Chemicals

Aniline (Riedel de Haen) was vacuum-distilled before use. Methylene chloride (Riedel de Haen), used for preparing poly-

merization solutions, was kept under a nitrogen atmosphere. Tetra-*n*-butylammonium perchlorate (TBAP), used as supporting electrolyte in nonaqueous medium, was obtained by the reaction of tetra-*n*-butylammonium hydroxide (40% aqueous solution, Merck) with perchloric acid (BDH), and recrystallized from the 1:9 mixture of water and ethyl alcohol by volume for several times. It was then dried at 120°C under vacuum for 12 h and kept under nitrogen atmosphere. Doubly distilled water was used to prepare the aqueous solutions. Sulphate buffer solution (SBS) at pH 4 was prepared using NaHSO_4 (Merck) and Na_2SO_4 (Merck). Phenolic solutions prepared in SBS at pH 4 were deoxygenated by bubbling pure nitrogen gas (BOS) prior to the use in electrochemical experiments.

Electrochemical Cell and Electrodes

The electrochemical cell had five inlets, three of which were used for the electrodes and the other two for nitrogen gas inlet and outlet. In methylene chloride, the reference and counter electrodes were Ag/AgCl (sat) and Pt spiral in separate compartments, containing methylene chloride/100 mM TBAP solution, respectively. In aqueous medium, a saturated calomel electrode (SCE) was used as the reference electrode and a Pt wire electrode was used as the counter electrode. Working electrode was a Pt disc electrode ($A = 7.85 \times 10^{-3} \text{ cm}^2$) for the cyclic voltammetric studies. Before each experiment, the working electrode was polished with alumina (5.0 μm), then rinsed with twice-distilled water, cleaned in ultrasonic bath and dried. Finally, the electrode was washed with methylene chloride, and dried before use. Macro polymer films were prepared on a Pt foil ($A = 1.0 \text{ cm}^2$). This electrode was cleaned by being held in flame for a few minutes. The electrodes were rinsed with methylene chloride and dried before use. Electrochemical studies were carried out with CH Instruments System, Model 660B.

Synthesis of PVF^+ -PANI Composite and Its Homopolymer Films

Poly(vinylferrocene) (PVF) was synthesized using the method of chemical polymerization of vinylferrocene (Aldrich).²⁷ The green-colored $\text{PVF}^+(\text{ClO}_4^-)$ redox polymer was synthesized on Pt disc electrode in methylene chloride solution containing 100 mmol L^{-1} TBAP/1.0 mg mL^{-1} of PVF using potentiodynamic method. When the potential range was applied from -0.20 to 1.80 V [versus Ag/AgCl (sat)], green-colored $\text{PVF}^+(\text{ClO}_4^-)$ film was not observed on Pt electrode because of its reduction to PVF and thus being stripped from the electrode surface by dissolution in methylene chloride.¹⁴ Nevertheless, the green $\text{PVF}^+(\text{ClO}_4^-)$ film can be easily obtained on Pt disc electrode surface when the lower potential is chosen as 0.20 V instead of -0.20 V.¹⁴ Therefore, PVF^+ -PANI composite-coated Pt electrode was prepared in 100 mM TBAP/33.0 mM HClO_4 /1.0 mg mL^{-1} PVF/100 mM aniline monomer solution by sweeping the potential region between 0.20 and 1.80 V [versus Ag/AgCl (sat)], at a scan rate of 100 mV s^{-1} . For comparison, PANI-coated electrode was also prepared in a methylene chloride solution, containing 100 mM TBAP/33.0 mM HClO_4 /50.0 mM aniline monomer under the same condition.

The polymerization solutions were deoxygenated by bubbling pure nitrogen gas before electrochemical coating. Ultraviolet-

visible (UV-vis) spectra were recorded at room temperature on a Double Beam PC8 Scanning Auto Cell UVD-3200 spectrophotometer. Fourier Transform Infrared (FTIR) spectra of the polymer coatings were recorded directly with a Perkin Elmer Spectrum One B spectrometer with ATR attachment.

Theoretical Calculation for Hydrogen Bonding

Theoretical calculations were performed by using the semiempirical (AM1) method^{28,29} in the HYPERCHEM 6.0 package, and a Pentium III 600 MHz computer. These methods were used to investigate the aromatic character of compounds^{30,31} and to study some complex structures such as polymers.³²⁻³⁴ The hydrogen bond lengths were calculated using the molecular mechanic MM2 method in Chem3D. In the calculations of the total energies (TE) and heats of formation (H_f), semiempirical AM1 method was used.

RESULTS AND DISCUSSION

Phenolic Compounds

The Effects of Intermolecular Hydrogen Bonding on the Electro-Oxidation Behavior of Phenolic Compounds. Figure 1(a-d) shows the cyclic voltammograms of Ph, Ct, Rs, and Hq recorded on bare Pt electrode in the SBS at pH 4. Broad oxidation peaks of Ph, Ct, Rs, and Hq are observed at about 0.90, 0.70, 0.85, and 0.55 V (versus SCE), respectively. When the cyclic voltammogram is taken from SBS, including 5.00 mM of Ph, Ct, Rs, and Hq at pH 4 each, a broad oxidation peak appears after 0.40 V instead of their individual peaks. This may be due to the forming of hydrogen-bonded oligomeric clusters, established by different phenolic molecules in this medium. The involvement of the various chain lengths in such oligomeric clusters may cause the oxidation peak to broaden. The solutions were also prepared by mixing Ph, Ct, Rs, and Hq solutions with a different sequence, and their voltammograms were recorded. Supporting Information, Table S1 lists the peak potentials and the peak currents, measured from these voltammograms. As seen in the table, the oxidation peak potentials and peak intensities are different in each case. Furthermore, the solution was prepared in the way in which the weighed solids of phenolic compounds were mixed in a beaker and then the mixture was dissolved in SBS. The concentration of each compound was 5.00 mM. The cyclic voltammogram of this mixture is given in Figure 1(e). The oxidation peak potential and its intensity are different from those of other quaternaries, as presented in Supporting Information, Table S1. Consequently, the variable results, obtained from the same solution that was prepared in different ways, indicate that all phenolic species are able to form the intermolecular hydrogen bond with each other. Supporting Information, Table S1 shows the results obtained from the cyclic voltammograms recorded from SBS, containing two of the phenolic species. Instead of their individual peaks, broad oxidation peaks appear, which is similar to the quaternaries. Therefore, it can be concluded that various hydrogen-bonded oligomeric clusters may form depending on the solution prepared in different ways.

The phenolic molecules are oxidized to their cation radicals at their own oxidation potentials. The cation radicals are converted into their radicalic species by losing one mole proton in aque-

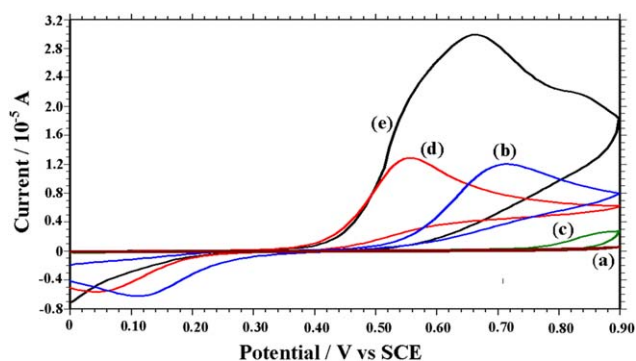
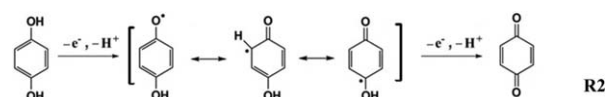
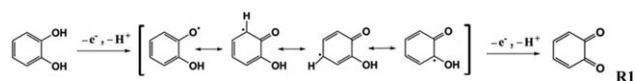
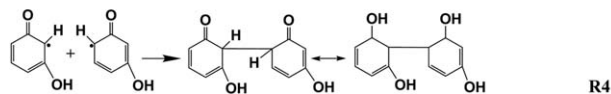
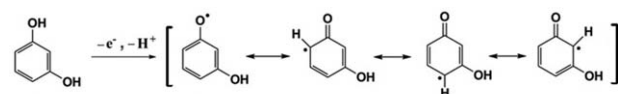
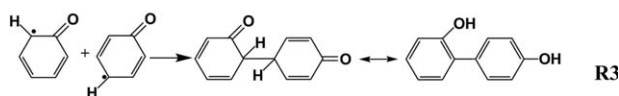
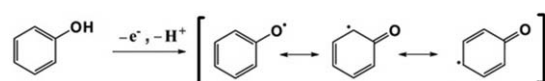


Figure 1. The cyclic voltammogram of 5.00 mM of (a) Ph, (b) Ct, (c) Rs, and (d) Hq in sulphate buffer solution (SBS) at pH 4; (e) a solution prepared mixing the solids of Ph + Rs + Ct + Hq in SBS at pH 4, $c_{\text{phenolic compound}} = 5.00 \text{ mM}$, scan rate (ν) = 100 mV s^{-1} . [Color figure can be viewed in the online issue, which is available at wileyonlinelibrary.com.]

ous solution. Radicalic species of Ct and Hq, whose radicalic center can be positioned on the carbon conjoint with oxygen atom in resonance form are oxidized once more at their own oxidation potentials. The resulting products are their quinoid structures as seen in the following equations.^{35,36}



Conversely, the radicalic species of Ph and Rs combine and form their dimers as the examples indicated in the following equations.³⁷⁻³⁹



The Effects of Intermolecular Hydrogen Bonding on the Spectroscopic Behavior of Phenolic Compounds. The effect of intermolecular hydrogen bonding on the spectroscopic behavior

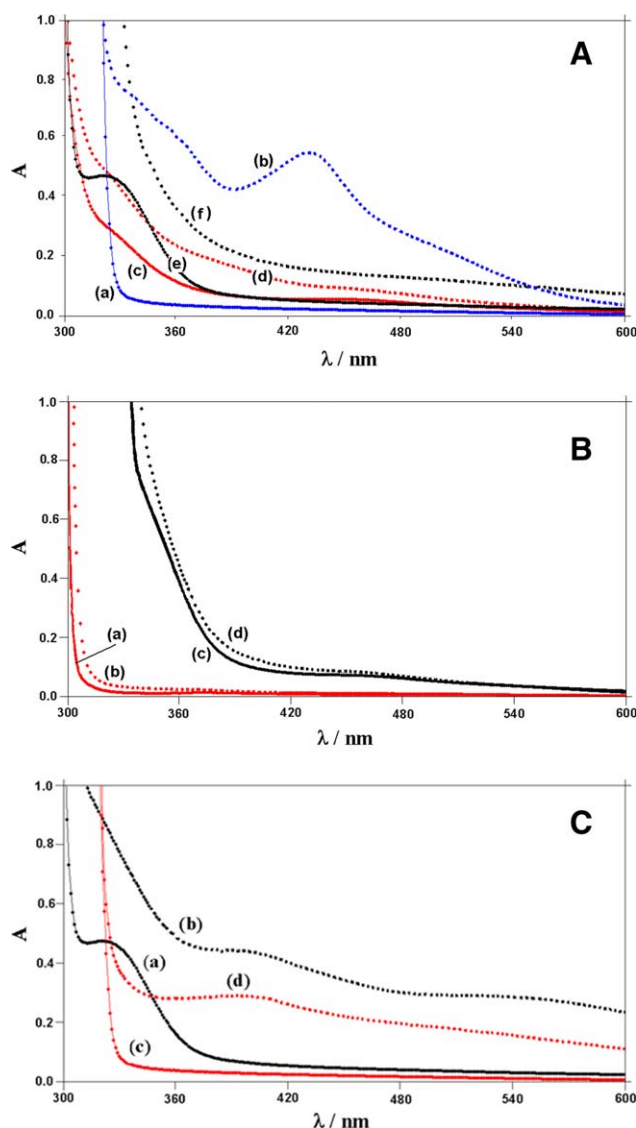


Figure 2. (A) UV-vis spectra of (a) Hq, (c) Rs, and (e) Ct solutions freshly prepared in nitrogen atmosphere at pH 4; and the same solutions (b) Hq, (d) Rs, and (f) Ct left to open air for 30 min. (B) UV-vis spectra of (a) 500 mM Ph solution (c) a solution freshly prepared mixing from the solids of Ph + Rs + Ct + Hq in nitrogen atmosphere at pH 4 (SBS); and the same solutions (b) Ph (d) Ph + Rs + Ct + Hq left to open air for 30 min. (C) UV-vis spectra of (a) Ct and (c) Hq solutions freshly prepared in nitrogen atmosphere at pH 4 (SBS); and the same (b) Ct and (d) Hq solutions after being immersed of PANI film for 30 min in nitrogen atmosphere, $c_{\text{each phenolic compound}} = 500$ mM. [Color figure can be viewed in the online issue, which is available at wileyonlinelibrary.com.]

was investigated. Each phenolic compound was dissolved in SBS at pH 4, and their colorless solutions were left in open air for 24 h to be oxidized by oxygen. It was observed that the colors of Ph and Ct solutions did not change. On the other hand, the Rs and Hq solutions turned into pale yellow and brown, respectively. Figure 2(A,B) shows the UV-vis spectra of the phenolic solutions before and after this treatment. The new peak was observed at 330 nm in the UV-vis spectra for Hq solution, compared to that of freshly prepared clear solution [Figure

2(Aa,b)]. Also, the absorption intensity in UV and vis regions increases for Rs solution [Figure 2(Ac,d)]. This might be due to the oxidation of Hq to benzoquinone and the oxidation of Rs to oligomeric species, respectively. Although the color of Ct solution did not change after treatment, it is clear that the spectrum in the UV region is different [Figure 2(Ae,f)]. The UV-vis spectrum of Ph solution did not change after being left in open air as seen in Figure 2(Ba,b). In the case of the solution prepared by mixing the solids from each phenolic compound, the uncolored solution (and also the UV-vis spectrum) did not change after being left in open air [Figure 2(Bc,d)]. In other words, Hq, Rs, and Ct in this solution were not oxidized by oxygen in the air, unlike their individual solutions. This is an evidence for the fact that the phenolic molecules are bound by intermolecular hydrogen bonding. The oxidations of Hq, Rs, and Ct molecules are hindered by the bonding of different phenolic molecules.

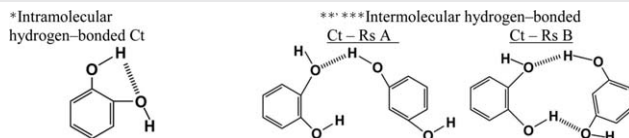
Theoretical Calculations for Hydrogen Bonding. To investigate the formation of the hydrogen bonding between phenolic compounds, theoretical calculations were performed using Chem3D and semiempirical Austin Model 1 (AM1). Table I shows the probable hydrogen-bonded monomers and dimers of phenolic compounds, and their heats of formation (H_f), total energies (TE), and hydrogen bond lengths. Here, A and B represent the single and double hydrogen-bonded dimers, respectively (Table I and Supporting Information, Schema S1). ΔH_f value is the difference between the H_f value of hydrogen-bonded dimer and the total H_f values of its monomers such as $\Delta H_f = [H_f(\text{Rs} - \text{Hq})] - [H_f(\text{Rs}) + H_f(\text{Hq})]$ for Rs-Hq A molecule. The negative sign shows that the hydrogen-bonded dimer is more stable than its monomers. The inspection of the values in Table I leads to the prediction that the intermolecular hydrogen-bonded dimers are most probably formed instead of intramolecular hydrogen-bonded monomers, since ΔH_f and TE values are minimal in such dimers. When A and B type hydrogen-bonded dimers are compared, it can be seen that single hydrogen bonding (A type) is preferred. The hydrogen bond length values also support the feasibility of the formation of hydrogen bonds.⁴⁰⁻⁴² Consequently, it can be suggested that the hydrogen-bonded dimers, trimers, and oligomeric clusters are formed among the same and/or different phenolic molecules. This result is compatible with that of UV-vis and cyclic voltammogram obtained above.

PANI

To combine the electrocatalytic properties of intrinsically conducting polymer and redox polymer, the PVF⁺-PANI composite-coated electrode is prepared electrochemically and its performance is examined in the amperometric determination of Ct and TotPh compounds. At first, the interaction of phenolic molecules with its homopolymers (PANI and PVF⁺) is investigated spectroscopically, voltammetrically, and theoretically. Therefore, PANI-coated electrode was prepared in a methylene chloride solution, containing aniline monomer and HClO₄ by sweeping the potential region between 0.20 and 1.80 V [versus Ag/AgCl (sat)], at a scan rate of 100 mV s⁻¹.

Table I. Heats of formation and Hydrogen Bond Lengths Calculated by Using AM1 Method and Total Energy Values Calculated Using *ab initio* (STO-3G) Method for the Phenolic Molecules and Their Intramolecular and Intermolecular Hydrogen-Bonded Species

	H_f (kcal mol ⁻¹)	ΔH_f	Hydrogen bond length (Å)		TE (kcal mol ⁻¹)
			Intramolecular	Intermolecular	
Ph	-22.4085				-27003.15
Ph-Ph A	-47.8839	-3.07		2.177	-54009.36
Ct	-66.4930				-34396.37
*Ct	-66.8628	-0.37	2.256		-34396.74
Ct-Ct A	-137.431	-4.44		2.170	-68797.19
Ct-Ct B	-137.291	-4.31		2.150 (2.99)	-68797.05
Rs	-66.9661				-34396.85
Rs-Rs A	-137.280	-3.34		2.175	-68797.04
Rs-Rs B	-136.841	-2.91		2.313 (3.780)	-68796.60
Hq	-66.1631				-34396.04
Hq-Hq A	-135.738	-3.41		2.187	-68795.50
Hq-Hq B	-132.846	-0.52		5.293 (4.984)	-68792.61
Ph-Ct A	-91.9069	-3.00		2.178	-61402.52
Ph-Rs A	-92.0592	-2.68		2.180	-61402.68
Ph-Hq A	-91.2187	-2.65		2.191	-61401.84
**Ct-Rs A	-136.017	-2.56		2.159	-68795.77
Ct-Hq A	-133.868	-1.21		2.266	-68793.63
Rs-Hq A	-136.319	-3.19		2.168	-68796.08
***Ct-Rs B	-131.427	2.03		2.366 (2.366)	-68791.19
Ct-Hq B	-132.541	0.12		4.898 (4.154)	-68792.30
Rs-Hq B	-135.446	-2.32		2.983 (4.753)	-68795.20



A and B represent single and double hydrogen-bonded dimers, respectively. (The structure of monomers and dimers are given for Ct in the table as an example. Look at Supporting Information, Schema S1 for other structures.)

Fourier Transform Infrared. The immobilization of phenolic molecules in PANI polymer was investigated by FTIR measurement. PANI films, deposited on Pt electrode, were immersed in 500 mM Ph, Ct, Rs, and Hq solutions under nitrogen atmosphere for 30 min. Then, they were immersed in the phenolic compound-free SBS, so that this compound adsorbed on electrode surface was removed. This cleaning procedure was repeated three times to remove residual phenolic compounds. Figure 3(A) shows the FTIR spectra of the films before and after this treatment.

First, FTIR spectrum of PANI polymer is characterized. This spectrum shows the characteristics similar to the literature reports^{43–45} with vibration bands of a doped polyaniline structure. The spectrum of PANI polymer shows main peaks at about 1561 and 1492 cm⁻¹, corresponding to quinone and benzene ring-stretching deformations, respectively.⁴³ The band characteristic of the conducting protonated form is observed at 1243 cm⁻¹ and is interpreted as a —C—N⁺ stretching vibration in the polaron structure.⁴³ The absorption peaks at 742 and 1142 cm⁻¹ are assigned to —C—H bending outside and inside

of plane, respectively.⁴⁶ Out-of-plane bending deformations of —C—H on 1,4 disubstituted rings are located in the region of 800–880 cm⁻¹.⁴⁷ The broad band at 1083 cm⁻¹ is related to positive charges in the polymer chains.⁴⁸ The peak at 625 cm⁻¹ is also assigned to Cl—O stretching due to ClO₄⁻.⁴⁸

Second, the FTIR spectra of PANI polymers, immersed one by one in Ph, Ct, Rs, and Hq solutions, are also evaluated [Figure 3(A)]. As seen in these spectra, an additional peak together with the peaks of PANI polymer is observed at 1385 cm⁻¹,⁴⁹ after being immersed in phenolic solutions. When compared to the spectra of phenolic molecules, this peak might belong to in-plane O—H bending in phenolic molecules, which means that the phenolic molecules do not remove the polymer structure after cleaning. This experimental result proves that the phenolic molecules are immobilized on the polymer matrix.

UV-vis. When PANI films deposited on Pt foil electrodes were separately immersed in the colorless phenolic solutions (the concentration of each solution is 500 mM) under nitrogen atmosphere, it was observed that the colors of Ph and Rs

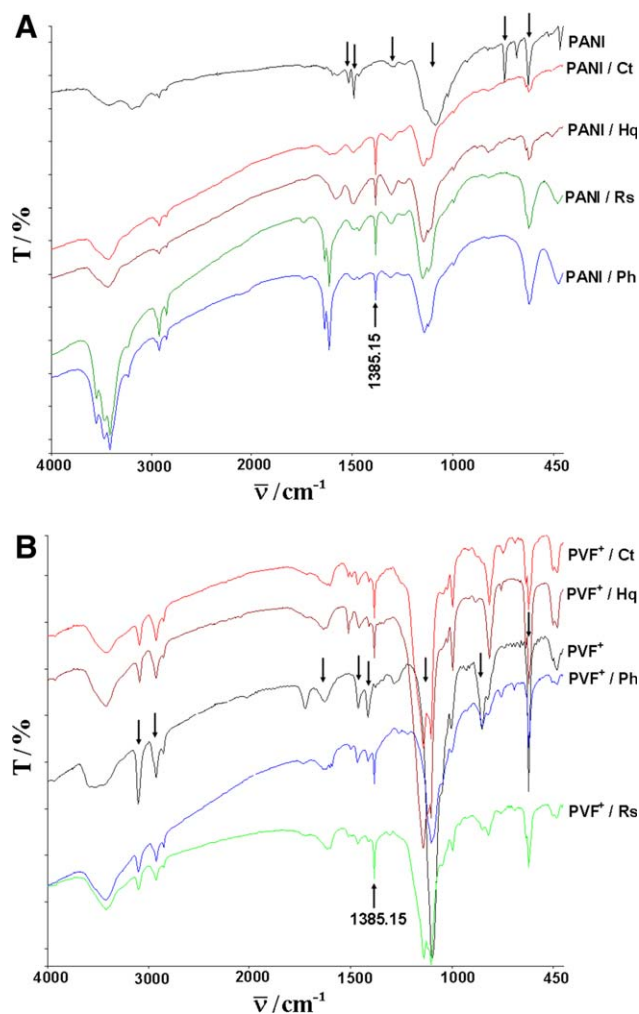


Figure 3. (A) FTIR spectra of PANI coatings before and after being immersed in Ph, Rs, Ct, and Hq solutions at pH 4 in nitrogen atmosphere. (B) FTIR spectra of PVF⁺ coatings before and after being immersed in the Ph, Rs, Ct, and Hq solutions at pH 4 in nitrogen atmosphere, $c_{\text{phenolic compound}} = 500$ mM. [Color figure can be viewed in the online issue, which is available at wileyonlinelibrary.com.]

solutions did not change. On the other hand, the color of solutions containing Ct and Hq turned into pink and yellow after treatment, respectively. The UV–vis spectra of these solutions before and after immersion were taken [Figure 2(C)]. When these spectra are compared with the UV–vis spectra of Ct and Hq solutions that were left in open air to be oxidized by oxygen [Figure 2(A)], the color changes could be interpreted as oxidation. Ct and Hq molecules might be chemically oxidized to their quinoid structures by quinoid structure of PANI chains.⁵⁰

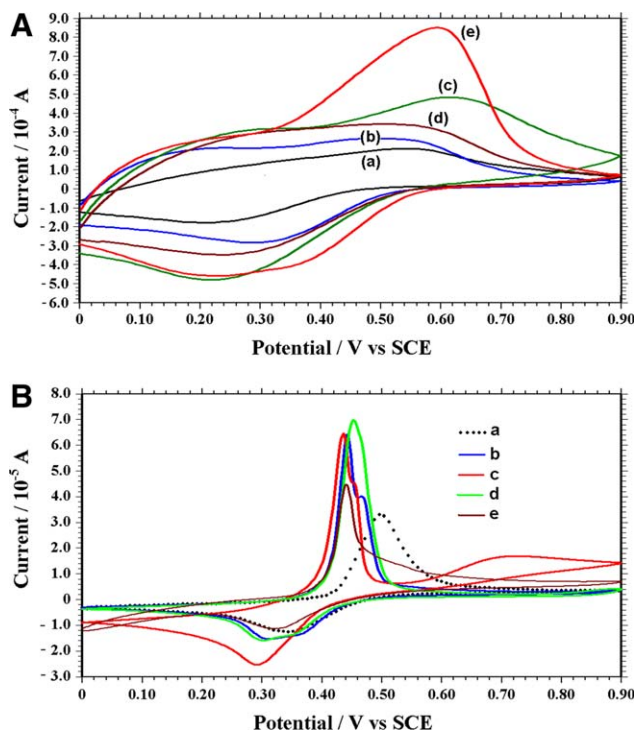
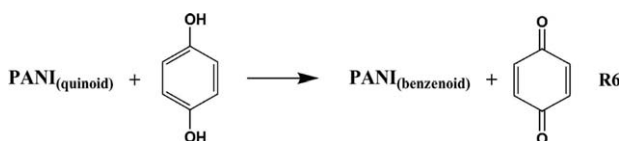
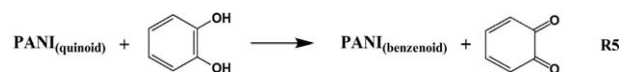


Figure 4. (A) Cyclic voltammograms recorded in SBS at pH 4 for (a) PANI film and PANI films having been immersed in SBS containing (b) Ph, (c) Ct, (d) Rs, and (e) Hq, $\nu = 100$ mV s⁻¹. (B) Cyclic voltammograms recorded in SBS at pH 4 for (a) PVF⁺ film and PVF⁺ films after being immersed in SBS containing (b) Ph, (c) Ct, (d) Rs, and (e) Hq at pH 4, $c_{\text{phenolic compound}} = 5.00$ mM, $\nu = 100$ mV s⁻¹. [Color figure can be viewed in the online issue, which is available at wileyonlinelibrary.com.]

In other words, these reactions provide the catalytic oxidation of Ct and Hq molecules which also hinder the overoxidation of PANI polymer in aqueous solution during the amperometric measurement.

Cyclic Voltammetry. The chemical reaction between PANI and phenolic compounds stated above was also investigated by cyclic voltammetry. PANI films deposited on Pt electrode were separately immersed in 500 mM Ph, Ct, Rs, and Hq solutions at pH 4 under nitrogen atmosphere for 30 min and then immersed in the phenolic compound-free SBS so that this compound adsorbed on electrode surface was removed. Figure 4(A) shows the cyclic voltammograms recorded in SBS at pH 4 for these films after treatment and nontreatment of PANI film for comparison. As seen in this figure, the electroactivities of PANI films are significantly enhanced in the case of Ct and especially Hq. This is an evidence for the fact that the quinoid structures of PANI chains are chemically reduced to the benzenoid structures by Ct and Hq molecules.

Theoretical Calculations. Theoretical calculations are also performed to estimate whether there is hydrogen bonding between phenolic molecules and PANI. Table II shows the probable hydrogen-bonded species and their heats of formation, total energies, and hydrogen bond lengths. The results show the feasibility of the formation of hydrogen bonds from both imine and

Table II. Heats of formation and Hydrogen Bond Lengths Calculated by Using AM1 Method and Total Energy Values Calculated through *ab initio* (STO-3G) Method for PANI and Its Hydrogen-Bonded Dimers with Phenolic Compounds

	H_f (kcal mol ⁻¹)	ΔH_f	Hydrogen bond length (Å)	TE (kcal mol ⁻¹)
Ph	-22.4085			-27003.15
Ct	-66.4930			-34396.37
Rs	-66.9661			-34396.85
Hq	-66.1631			-34396.04
PANI	167.755			-101317.57
PANI(amine)-Ph	144.316	-45.850	2.773	-128321.75
PANI(imine)-Ph	143.422	-46.940	2.570	-128322.65
*PANI(amine)-Ct	99.4561	-133.34	2.774	-135715.75
**PANI(imine)-Ct	100.504	-131.91	2.774	-135714.70
PANI(amine)-Rs	100.897	-133.83	2.762	-135714.68
PANI(imine)-Rs	98.3012	-136.42	2.730	-135716.27
PANI(amine)-Hq	100.926	-132.99	2.767	-135714.28
PANI(imine)-Hq	99.7373	-134.18	2.671	-135715.47

*PANI(amine) - Ct:

**PANI(imine) - Ct:

The structure of hydrogen-bonded monomer and dimers are given for Ct in the table as an example.

amine centers of PANI. A comparison of the calculated ΔH_f , TE, and hydrogen bond lengths for the hydrogen-bonded species reveals that hydrogen bonding preferably occurs on imine centers of PANI for Ph, Rs, and Hq molecules. However, it occurs on amine centers for Ct. Most importantly, it can be concluded that phenolic molecules are immobilized into both imine and amine centers of the PANI chain.

PVF⁺

The interaction of phenolic molecules with PVF⁺ polymer is also investigated spectroscopically and voltammetrically. Therefore, PVF⁺-coated electrode was prepared in a methylene chloride solution containing PVF polymer and HClO₄ by sweeping the potential region between 0.20 and 1.80 V [versus Ag/AgCl (sat)], at a scan rate of 100 mV s⁻¹.

Fourier Transform Infrared. PVF⁺ films deposited on Pt electrode were immersed in 500 mM Ph, Ct, Rs, and Hq solutions at pH 4 under nitrogen atmosphere for 30 min and then immersed in the phenolic compound-free SBS, so that this compound adsorbed on electrode surface was removed. Figure 3(B) shows the FTIR spectra of the films before and after these treatments. First, FTIR spectrum of PVF⁺ polymer is characterized. In the spectrum, the following characteristic peaks appear: —C=C— skeleton stretching in aromatic structure at 1419, 1466, and 1632 cm⁻¹; aromatic —C—H out-of-plane bending at 870 cm⁻¹; aliphatic —C—H stretching at 2851 and 2923 cm⁻¹; —C—H stretching in aromatic pentadienyl cycle at 3100 cm⁻¹.^{46,51} The broad band at 1083 cm⁻¹ is related to positive charges in the polymer chains.⁴⁸ The peak at 625 cm⁻¹ is also assigned to Cl—O stretching due to ClO₄⁻.⁴⁸ Second, the FTIR spectra of PVF⁺ polymers, each being separately

immersed in Ph, Ct, Rs, and Hq solutions, are also evaluated [Figure 3(B)]. A comparison of FTIR spectra of the films before and after the treatments reveals that an additional peak with the peaks of PVF⁺ polymer was clearly observed at 1385 cm⁻¹,⁴⁹ which was in-plane —O—H bending after being immersed in the phenolic solutions, as in the case of PANI polymer. To put it differently, all the phenolic molecules were also immobilized into PVF⁺ polymer.

UV-vis. PVF⁺ films deposited on Pt foil electrodes were separately immersed in the colorless phenolic solutions (the concentration of each solution is 500 mM) under nitrogen atmosphere. The green-colored PVF⁺-coated electrode turned into yellow after being immersed in the phenolic solutions, and fragments of the film also peeled off at places on the electrode surface. On the other hand, it was observed that the colors (and also the UV-vis spectra) of phenolic solutions did not change after treatment. This means that Ct and Hq molecules are not oxidized by PVF⁺ polymer, unlike those of PANI polymer.

Cyclic Voltammetry. Electrochemical behavior of phenolic compounds on PVF⁺-coated electrode was also investigated. Figure 4(B) shows the cyclic voltammograms of PVF⁺ films taken as soon as they were immersed in SBS solutions containing phenolic compounds at pH 4 without the film being peeled off at places from the electrode surface. For comparison, the cyclic voltammogram of PVF⁺-coated electrode is given in the same figure [Figure 4(Ba)]. It is clear from the comparison of these cyclic voltammograms that the oxidation of the PVF shifted to lower potentials while also increasing its intensity in the presence of phenolic compounds. Consequently, it can be suggested that iron ions in ferrocene moieties of PVF⁺ could form

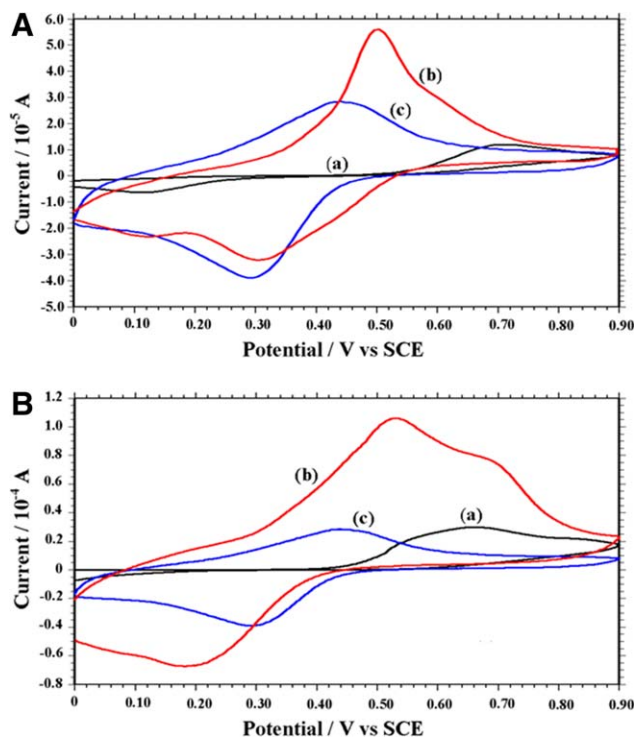


Figure 5. (A) Cyclic voltammogram of 5.00 mM Ct in SBS at pH 4 (a) on bare Pt electrode, (b) on PVF⁺-PANI-coated electrode, and (c) electrochemical behavior of PVF⁺-PANI film. (B) Cyclic voltammogram of 20.0 mM TotPh in SBS at pH 4 (a) on bare Pt electrode, (b) on PVF⁺-PANI-coated electrode, and (c) electrochemical behavior of PVF⁺-PANI film in SBS at pH 4, $\nu = 100 \text{ mV s}^{-1}$. [Color figure can be viewed in the online issue, which is available at wileyonlinelibrary.com.]

complex structures with —OH group in the phenolic molecules. In the literature, it was demonstrated that some phenolic species form chelate ions with Fe²⁺ and Fe³⁺ ions.⁵² Thus, it can be concluded that concentration of phenolic compounds increases on the electrode surface due to the formation of complex.

PVF⁺-PANI Composite

PVF⁺-PANI composite-coated electrode was electrochemically prepared by codepositing PANI and PVF⁺ polymers on Pt electrode in a methylene chloride solution containing PVF polymer, aniline monomer, and HClO₄.¹⁴ Supporting Information, Figure S1 shows the cyclic voltammetric scans taken during deposition in the potential region between 0.20 and 1.80 V [versus Ag/AgCl (sat)]. Aniline monomer and PVF polymer are oxidized at about 1.30 and 0.50 V [versus Ag/AgCl (sat)] in this medium, respectively.¹⁴ Therefore, PANI and PVF⁺ polymers are simultaneously deposited and encapsulated within each other as a mixture during the deposition of the composite film. The encapsulation of PVF⁺ polymer inside the growing PANI polymer provides the retainment of PVF⁺ on the electrode surface even if the polymer forms complex structures with phenolic molecules during immersion.

Determination of Catechol and Total Phenolic Compounds. Dark-green-colored PVF⁺-PANI composite-coated electrode was examined for the determination of Ct and TotPh because of the

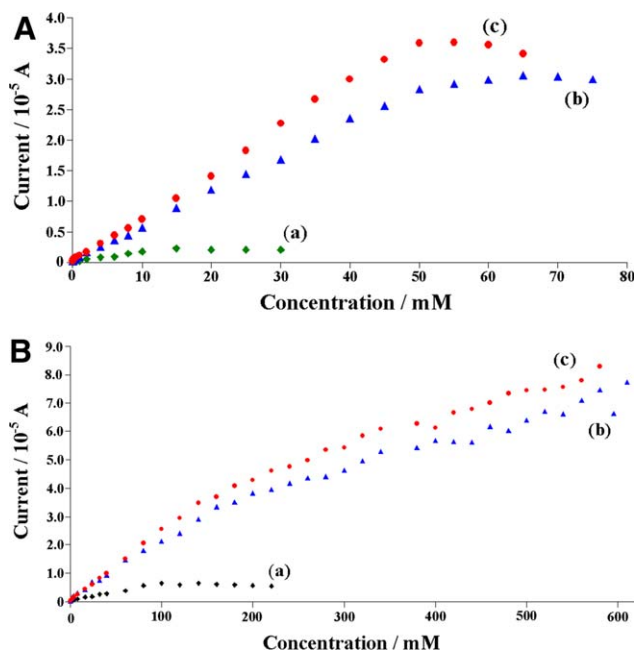


Figure 6. (A) Influence of Ct concentration on current value measured at optimum conditions for (a) bare Pt electrode (at 0.72 V), (b) PANI-coated (at 0.55 V), and (c) PVF⁺-PANI composite-coated (at 0.50 V) Pt electrodes. (B) Influence of TotPh concentration on current value measured at optimum conditions for (a) bare Pt electrode (at 0.68 V), (b) PANI-coated (at 0.60 V), and (c) PVF⁺-PANI composite-coated (at 0.45 V) Pt electrodes. [Color figure can be viewed in the online issue, which is available at wileyonlinelibrary.com.]

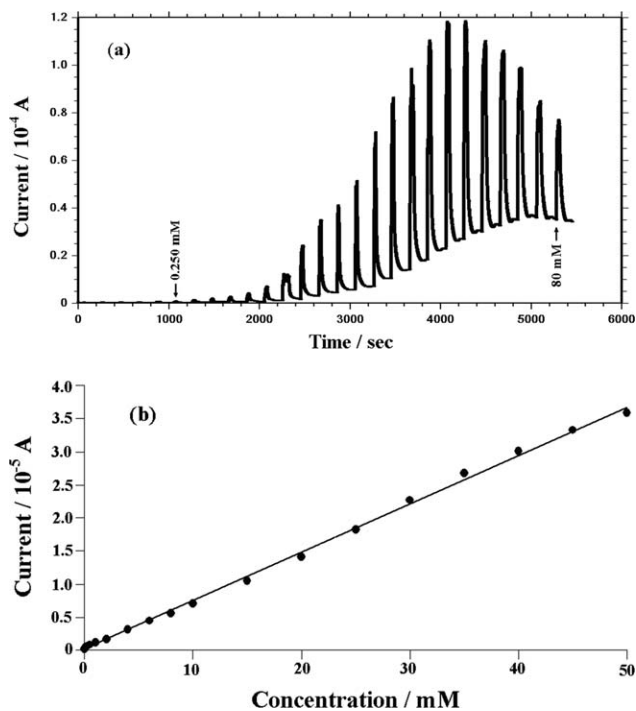


Figure 7. (a) Amperometric $I-t$ curve recorded at 0.50 V (versus SCE) on the successive additions of various Ct concentrations over PVF⁺-PANI coating obtained from the methylene chloride/100 mM TBAP solution containing 1.00 mg/mL PVF, 100 mM aniline, and 33.0 mM HClO₄ (b) its calibration curve for linearity range of Ct concentration.

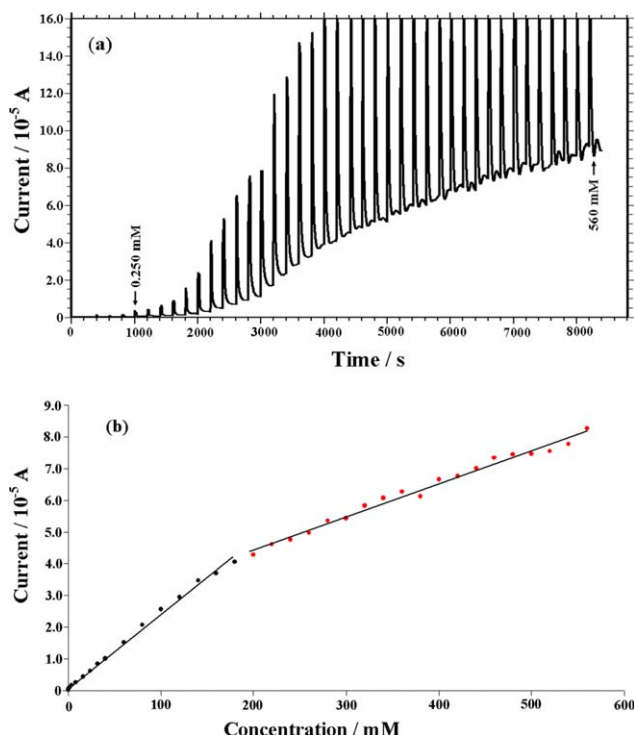


Figure 8. (a) Amperometric $I-t$ curve recorded at 0.45 V (versus SCE) on the successive additions of various TotPh concentrations over PVF⁺-PANI coating obtained from the methylene chloride/100 mM TBAP solution containing 1.00 mg/mL PVF, 100 mM aniline, and 33.0 mM HClO₄ (b) its calibration curve for linearity range of TotPh concentration. [Color figure can be viewed in the online issue, which is available at wileyonlinelibrary.com.]

importance of their quantitative analysis in the pharmaceuticals and environmental areas, respectively. The construction of hydrogen bonds by PANI and complexation by PVF⁺ ensure immobilization of phenolic molecules into both polymers in the composite film as indicated above. PVF⁺ polymer can also work as an electron transfer mediator in the composite film. Thus, it is expected that the concentrations of the phenolic compounds increase on the electrode surface. Figure 5(A,B) shows the feasibility of this expectation. As seen in these figures, the oxidation peak intensities of Ct and TotPh significantly increase on composite-coated electrodes [Figure 5(Ab,Bb)] when compared to those of bare Pt and solely composite coating.

The responses of composite-coated electrodes to Ct and TotPh were investigated by using amperometric $I-t$ method in SBS at pH 4 and compared to those of PANI-coated and bare Pt electrodes. PVF⁺-coated electrode could not be used because of the partial peeling off the film from the electrode surface during amperometric measurements. The applied potentials varying between 0.45 and 0.60 V (versus SCE) were examined for amperometric determination in an unstirred solution, and optimum potentials were obtained for each electrode (Tables III and IV). The steady-state current values recorded at their optimum potentials were plotted against the bulk concentration of Ct and TotPh using composite-coated electrode and also PANI-coated

and bare Pt electrodes for comparison [Figure 6(A,B)]. While low responses at bare Pt electrodes were observed, clear increases were obtained at PANI-coated electrodes as seen in these figures. The highest responses were observed at PVF⁺-PANI composite-coated electrodes at 0.45 and 0.50 V for Ct and TotPh, respectively. The amperometric curves and their calibration curves plotted in the linear concentration range are given in Figures 7 and 8 for the emphasized film, respectively. Tables III and IV show the analytical parameters obtained from these calibration curves besides those of PANI-coated and bare Pt electrodes. Limit of detection (LOD) and limit of quantification (LOQ) were calculated from the equations, 3 and 10 s/m , respectively,⁵³ “ s ” being calculated from the current responses of the lowest concentration that generate a measurable current in five replicate measurements.

As seen in Tables III and IV, the lowest potentials are determined as 0.50 and 0.45 V (versus SCE) on PVF⁺-PANI composite-coated electrode for Ct and TotPh, respectively. The lowest applied potentials and the highest responses indicate the stable catalytic properties of the PVF⁺-PANI composite coating. The responses could be conducted via two different mechanisms: since PVF⁺ forms complexation with phenolic molecules, PANI immobilized them by the hydrogen bonding as indicated above. In addition, PANI is chemically reduced by Ct and/or Hq due to the catalytic reaction (R5 and R6). Meanwhile, the reduced PANI is electrochemically oxidized at the applied potential for Ct and TotPh determination (0.50 and 0.45 V). Thus, polarons are regenerated in the PANI polymer. This reversible process

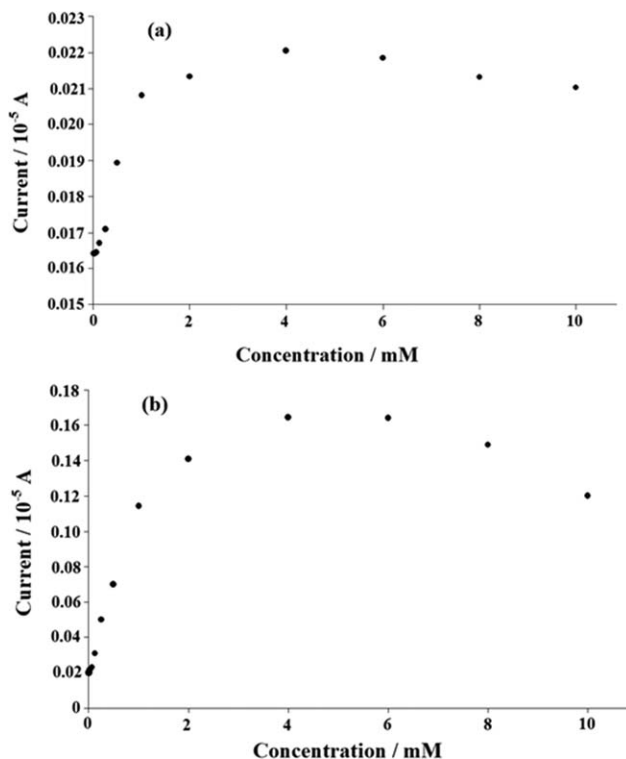


Figure 9. Influence of (a) Ph and (b) Rs concentrations on current values measured at their optimum conditions (at 0.55 V) for PANI-coated Pt electrode.

Table III. Analytical Parameters of Calibration Curves by Using Bare, PANI-Coated, and PVF⁺-PANI Composite-Coated Pt Electrodes for Determination of Ct

	Bare Pt	PANI-coated Pt	PVF ⁺ -PANI-coated Pt
Applied potential (V)	0.72	0.55	0.50
Sensitivity ($\mu\text{A mM}^{-1}$)	0.34	0.57	0.73
R^2	0.994	0.999	0.999
Linear range (mM)	3.48×10^{-3} –15.0	1.82×10^{-3} –50.0	1.35×10^{-3} –50.0
Limit of quantification (LOQ) (mM)	3.48×10^{-3}	1.82×10^{-3}	1.35×10^{-3}
Limit of detection (LOD) (mM)	1.04×10^{-3}	5.45×10^{-4}	4.05×10^{-4}

continuously occurs during amperometric measurement. As a result, the response of PANI-coated electrode is more sensitive and in a larger linear range in comparison to that of bare electrode. In addition, composite film is more sensitive than that of PANI for both Ct and TotPh determination. The linear response range obtained for Ct in this study is similar to that of electrode in the literature; tryptophan-functionalized graphene electrode (5.0×10^{-3} – 5.0×10^{-1} mM),⁵⁴ hexadecyl trimethyl ammonium bromide functionalized graphene oxide/multiwalled carbon nanotube modified electrode (1.0×10^{-1} – 4.0×10^{-1} mM),⁵⁵ poly(3-thiophenemalonic acid)-modified glassy carbon electrode (7.81×10^{-1} – 5.0×10^{-1} mM).⁵⁶ The linear response range obtained for TotPh in this study is similar to that of the electrode in the literature; modifying a glassy carbon electrode with composite film of graphene nanosheet and poly(4-vinylpyridine) (1.0×10^{-4} – 1.0×10^{-2} mM)⁵⁷ and electrospun carbon nanofiber-modified carbon paste electrode (1.0×10^{-3} – 2.0×10^{-1} mM).⁵⁸

As seen in Figure 6(B), both films (PANI and PVF⁺-PANI) have two linear fragments with different slopes for the determination of TotPh. This observation may arise from the presence of four different phenolic compounds in the TotPh solution because a similar property is not observed in the individual determination of Ct [Figure 6(A)] and Hq.⁵⁹ To determine the contributions of Ph and Rs to the response of TotPh, the amperometric *I*-*t* curves were recorded under their optimum conditions on PANI-coated electrodes. Figure 9 shows the variation of current with concentration for Ph and Rs. Their current values and linearity ranges are found to be so insignificant that

the contributions of Ph and Rs to the steady-state current of TotPh could be neglected [Figures 7(b), 8(b), and 9]. The small current values may arise from the coupling of cation radicals of Ph and Rs with polaron of PANI and it results in the degradation of PANI polymer. Therefore, it is possible to predict that the response of TotPh could be due to two-Ct and Hq-based essential hydrogen-bonded clusters. While the upper limits of linearity ranges were 50.0 mM for Ct (Table III) and 115 mM⁵⁹ for Hq, this value is, on the other hand, above 600 mM for TotPh due to the construction of intermolecular hydrogen bonds among phenolic compounds (Table IV). It is interesting that the intermolecular hydrogen bonding prevent degradation of PANI film even in the presence of Ph and Rs.

Reproducibility of Composite-Coated Electrode. The reproducibility of PVF⁺-PANI composite-coated electrode was examined for the determination of Ct and TotPh. Each measurement was carried out using the freshly prepared composite-coated electrode. Before each measurement, the composite-coated electrode was reduced at 0.20 V [versus Ag/AgCl (sat)] in blank solution for 10 min. The relative standard deviations (RSD) were 0.29% and 1.17% ($n = 5$) for 4.00 mM Ct and TotPh solutions, respectively. RSD were, on the other hand, 3.80% and 4.54% for 0.50 mM Ct and TotPh solutions, respectively. These results show that the reproducibility of electrode is reasonably high even if the responses were measured on the new coating in each case.

Reusability of Composite-Coated Electrode. The reusability of PVF⁺-PANI composite-coated electrode was also investigated over about a 5-week period. During this period, the prepared

Table IV. Analytical Parameters of Calibration Curves by Using Bare Pt, PANI-Coated, and PVF⁺-PANI Composite-Coated Pt Electrodes for Determination of TotPh

	Bare Pt	PANI-coated Pt	PVF ⁺ -PANI-coated Pt
Applied potential (V)	0.68	0.60	0.45
Sensitivity ($\mu\text{A mM}^{-1}$)	0.066	I: 0.20 II: 0.10	I: 0.24 II: 0.11
R^2	0.991	I: 0.996 II: 0.992	I: 0.996 II: 0.987
Linear range (mM)	1.13×10^{-2} –100.0	8.70×10^{-4} –180.0 and 180.0–560	4.10×10^{-4} –180.0 and 180.0–560
Limit of quantification (LOQ) (mM)	1.13×10^{-2}	8.70×10^{-4}	4.10×10^{-4}
Limit of detection (LOD) (mM)	3.38×10^{-3}	2.60×10^{-4}	1.23×10^{-4}

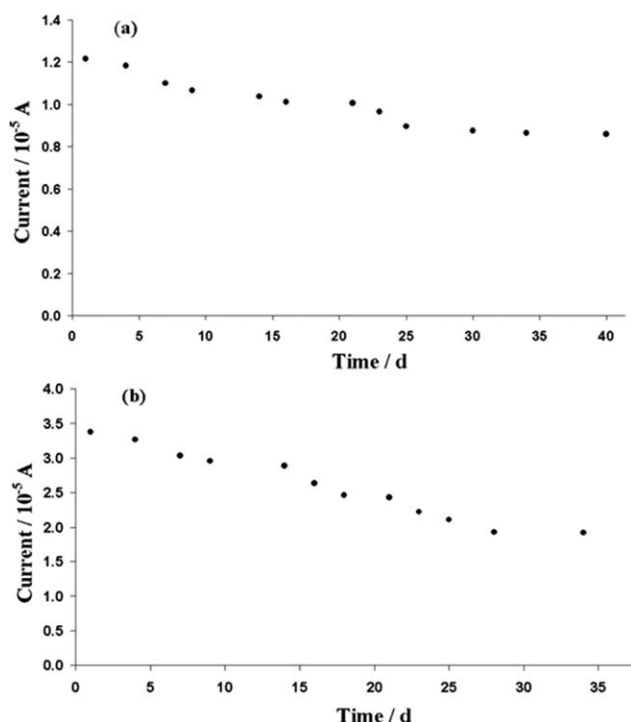


Figure 10. Long-term stability of PVF⁺-PANI coating for (a) Ct and (b) TotPh in SBS at pH 4 by using amperometric *I-t* method, $c_{\text{Ct, TotPh}} = 5.00$ mM.

electrodes were stored in nitrogen atmosphere. After measurements, the composite-coated electrode was immersed in SBS at pH 4 and then was reduced at 0.20 V [versus Ag/AgCl (sat)] for 10 min. Current values were measured at 0.50 and 0.45 V (versus SCE) for 5.00 mM Ct and TotPh solutions, respectively. The plot of current versus time was constructed (Figure 10). The current values gradually decreased up to 28 days after which the electrode responses nearly reached a steady-state current. As a result, this electrode preserved 70% and 60% of its initial responses for Ct and TotPh after reaching steady-state current, respectively. This may arise from the chemical reaction between Ct, Hq compounds, and PANI (R5, R6) as well as encapsulation of PVF⁺. Chemical reaction hinders the overoxidation of polymer by causing the continuous reduction of PANI. PVF⁺ should have reduced the electron transfer resistance of composite film.

CONCLUSIONS

This study demonstrates that the hydrogen bond formation among different phenolic compounds affects electro-oxidation and spectroscopic behaviors of phenolic compounds (Ph, Ct, Rs, and Hq). The oxidation behaviors of total phenolic compounds are different from their individual behaviors in sulphate buffer solution at pH 4 due to the existence of the intermolecular hydrogen-bonded dimers and/or oligomeric clusters. Intermolecular hydrogen bonding provides that the oxidations of Hq, Rs, and Ct molecules in TotPh are hindered by oxygen in air. Theoretical predictions, UV-vis, and FTIR evidences support the intermolecular hydrogen bonding. The interaction of the phenolic compounds with PANI and PVF⁺ homopolymer films are also investigated electrochemically and spectrosco-

ically. The results show that the phenolic molecules are immobilized in both polymers, due to the construction of hydrogen bonds by PANI and complexation with PVF⁺, which enhance determinations of Ct and TotPh. In addition, Ct and Hq are catalytically oxidized by PANI. Determinations of Ct and TotPh are examined on PVF⁺-PANI composite-coated Pt electrode by using amperometric *I-t* method because of the importance of their quantitative analysis in pharmaceuticals and environmental areas, respectively. Composite coating exhibits significant electrochemical activity toward Ct and TotPh in SBS at pH 4, with high sensitivity and a wide linearity range when compared to those of bare and PANI-coated Pt electrodes. The steady-state current versus the concentration is linear in the range of 1.35×10^{-3} –50.0 mM for Ct, and is fitted better with two linear regions, 4.10×10^{-4} –180 mM and 180–560 mM for TotPh and LOD is found to be 4.05×10^{-4} mM at 0.50 V and 1.23×10^{-4} mM at 0.45 V (versus SCE), respectively.

ACKNOWLEDGMENTS

Support of this work by Scientific Research Department of Hacettepe University (project no. 0801601011) is greatly appreciated. The authors wish to thank Şenay Saraç for her contribution.

REFERENCES

- Cleland, W. W.; Kreevoy, M. M. *Science* **1994**, *264*, 1887.
- Pekmez, N. O.; Can, M.; Yildiz, A. *Acta Chim. Slov.* **2007**, *54*, 131.
- Warshel, A. *Computer Modeling of Chemical Reactions in Enzymes and Solutions*; Wiley: New York, **1991**.
- Vianello, R.; Kovačević, B.; Ambrožič, G.; Mavri, J.; Maksić, Z. B. *Chem. Phys. Lett.* **2004**, *400*, 117.
- Li, X.; Chen, W.; Zhan, Q.; Dai, L.; Sowards, L.; Pender, M.; Naik, R. R. *J. Phys. Chem. B* **2006**, *110*, 12621.
- Li, A.; Zhang, Q.; Wu, H.; Zhai, Z.; Liu, F.; Fei, Z.; Long, C.; Zhu, Z.; Chen, J. *Adsorp. Sci. Technol.* **2004**, *22*, 807.
- Pan, B.; Xing, B. *Environ. Sci. Technol.* **2008**, *42*, 9005.
- Velhal, N.; Patil, N.; Jamdade, S.; Puri, V. *Appl. Surf. Sci.* **2014**, *307*, 129.
- Noufi, R.; Nozik, A. J.; White, J.; Warren, L. F. *J. Electrochem. Soc.* **1982**, *129*, 2261.
- Yano, J.; Ogura, K.; Kitani, A.; Sasaki, K. *Synth. Met.* **1992**, *52*, 21.
- Gülce, H.; Gülce, A.; Kavanoz, M.; Coşkun, H.; Yıldız, A. *Biosens. Bioelectron.* **2002**, *17*, 517.
- Gülce, H.; Celebi, S. S.; Özyörük, H.; Yıldız, A. *Pure Appl. Chem.* **1997**, *69*, 173.
- Gülce, H.; Özyörük, H.; Yildiz, A. *Electroanalysis* **1995**, *7*, 178.
- Kavanoz, M.; Şen, M.; Pekmez, N. *Collection Czechoslovak Chem. Commun.* **2011**, *76*, 1855.
- EPA method 604, Phenols in Federal Register, Friday October 26, **1984** Environmental Protection Agency Washington, DC, Part VIII, 40 CFR, Part 136, 58.

16. Bazrafshan, E.; Mostafapour, F. K.; Mansourian, H. J. *Health Scope* **1970**, *2*, 65.
17. Santana, C. M.; Ferrera, Z. S.; Padrón, M. E. T.; Rodríguez, J. J. S. *Molecules* **2009**, *14*, 298.
18. Castillo, M.; Domingues, R.; Alpendurada, M. F.; Barceló, D. *Anal. Chim. Acta* **1997**, *353*, 133.
19. Gatti, R.; Gioia, M. G.; Pietra, A. M.; Di, Cavrini, V. *Anal. Chim. Acta* **2001**, *447*, 89.
20. Naczka, M.; Shahidi, F. *J. Chromatogr. A* **2004**, *1054*, 95.
21. Ren, W.; Luo, H. Q.; Li, N. B. *Biosens. Bioelectron.* **2006**, *21*, 1086.
22. Li, C.; Liu, W.; Gu, Y.; Hao, S.; Yan, X.; Zhang, Z.; Yang, M. *J. Appl. Electrochem.* **2014**, *44*, 1059.
23. Liu, Y.; Wan, W.; Li, H. W. J.; Lu, X.; Liu, X. *J. Appl. Electrochem.* **2014**, *44*, 667.
24. Skládal, P.; Morozova, N. O.; Reshetilov, A. N. *Biosens. Bioelectron.* **2002**, *17*, 867.
25. Korkut, S.; Keskinler, B.; Erhan, E. *Talanta* **2008**, *76*, 1147.
26. Russell, I. M.; Burton, S. G. *Anal. Chim. Acta* **1999**, *389*, 161.
27. Smith, T. W.; Kuder, J. E.; Wychick, D. *J. Polym. Sci. Chem.* **1976**, *14*, 2433.
28. Dewar, M. J. S.; Yuan, Y. C. *Inorg. Chem.* **1990**, *29*, 3881.
29. Stewart, J. P. *J. Comput. Aid. Mol. Des.* **1990**, *4*, 1.
30. Baldridge, K. K.; Gordon, M. S. *J. Am. Chem. Soc.* **1988**, *110*, 4204.
31. Gestoso, P.; Brisson, J. *Comput. Theoret. Polym. Sci.* **2001**, *11*, 263.
32. Nyulászi, L.; Várnai, P.; Veszprémi, T. *J. Mol. Struct. THEOCHEM* **1995**, *358*, 55.
33. Copper, D. L.; Gerratt, J.; Raimondi, M. *Nature* **1986**, *323*, 699.
34. Fagerström, J.; Stafström, S. *Synth. Met.* **1997**, *85*, 1065.
35. Sotomayor, M. D. P. T.; Tanaka, A. A.; Kubota, L. T. *Anal. Chim. Acta* **2002**, *455*, 215.
36. Simic, A.; Manojlovic, D.; Segan, D.; Todorovic, M. *Molecules* **2007**, *12*, 2327.
37. Enache, T. A.; Oliveria-Brett, A. M. *J. Electroanal. Chem.* **2011**, *655*, 9.
38. Divi, R. L.; Doerge, D. R. *Biochemistry* **1994**, *33*, 9668.
39. Goto, H.; Furusho, Y.; Miwa, K.; Yashima, E. *J. Am. Chem. Soc.* **2009**, *131*, 4710.
40. Vianello, R.; Kovačević, B.; Ambrožič, G.; Mavri, J.; Maksić, Z. B. *Chem. Phys. Lett.* **2004**, *400*, 117.
41. Veyisoğlu, F.; Şahin, M.; Pekmez, N.; Can, M.; Yıldız, A. *Acta Chim. Slov.* **2004**, *51*, 483.
42. Zhang, J.; Wang, L.; Zhang, H.; Wang, R. *Synth. Met.* **2003**, *137*, 1349.
43. Blinova, N. V.; Stejskal, J.; Trchová, M.; Prokeš, J.; Omastová, M. *Eur. Polym. J.* **2007**, *43*, 2331.
44. Zhang, L.; Wan, M. *Nanotechnology* **2002**, *13*, 750.
45. Yang, J.; Ding, Y.; Chen, G.; Li, C. *Eur. Polym. J.* **2007**, *43*, 3337.
46. Stuart, B. *Infrared Spectroscopy: Fundamentals And Applications*; Wiley: New York, **2004**.
47. Khan, A.; Asiri, A. M.; Rub, M. A.; Azum, N.; Khan, A. A. P.; Khan, S. B.; Rahman, M. M.; Khan, I. *Compos. B Eng.* **2013**, *45*, 1486.
48. Pekmez, N.; Pekmez, K.; Yıldız, A. *J. Electroanal. Chem.* **1994**, *370*, 223.
49. Araujo, P. Z.; Morando, P. J.; Blesa, M. A. *Langmuir* **2005**, *21*, 3470.
50. Duić, L.; Grigić, S. *Electrochim. Acta* **2001**, *46*, 2795.
51. Pearce, P. J.; Bard, A. J. *J. Electroanal. Chem. Interf. Electrochem.* **1980**, *112*, 97.
52. Bugg, T. D. H.; Lin, G. *Chem. Commun.* **2001**, 941.
53. Long, G. L.; Winefordner, J. D. *Anal. Chem.* **1983**, *55*, 712A.
54. Jiang, H.; Zhang, D.; He, Z.; Lian, Q.; Xue, Z.; Zhou, X.; Lu, X. *Anal. Lett.* **2015**, *48*, 1426.
55. Yang, Y. J. W. L. *Nanotubes Carbon Nanostruct.* **2014**, *23*, 410.
56. Xu, G.; Tang, B.; Jing, S.; Tao, J. *Int. J. Electrochem. Sci.* **2015**, *10*, 10659.
57. Tehrani, R. M. A.; Ghadimi, H.; Ghani, S. A. *Sens. Actuators B Chem.* **2013**, *177*, 612.
58. Guo, Q.; Huang, J.; Chen, P.; Liu, Y.; Hou, H.; You, T. *Sens. Actuators B Chem.* **2012**, *163*, 179.
59. Kavanoz, M.; Pekmez, N. O. *J. Solid State Electrochem.* **2012**, *16*, 1175.